



## Mathematical Modeling and Sensitivity Analysis on Cadmium Transport in Kaolinite under Direct Current Electric Field

Milad Rezaee <sup>a\*</sup>, Mostafa Nasrollahi Gisel <sup>a</sup>, Saman Saffari <sup>b</sup>

<sup>a</sup> *Graduated Student in Geotechnical Engineering, Department of Civil Engineering, Kharazmi University, Alborz, Iran.*

<sup>b</sup> *Civil Engineering Department, Islamic Azad University, Malayer Branch, Hamedan, Iran.*

Received 3 September 2017; Accepted 30 October 2017

### Abstract

Soil pollution is a challenging concern for environmentalists. Different remediation methods have been proposed to remediate polluted soils. Most of the existing methods cannot purify low permeable soils. Electrokinetic remediation (EKR) is an effective method which can remediate fine-grained soils. Understanding the physicochemical phenomena of the EKR is necessary to achieve efficient experimental framework. Therefore, the present study aims to introduce a theoretical and mathematical model for the EKR process. In the present model, different transport phenomena including ion migration, electroosmotic flow, and diffusion were considered. In addition, Chemical reactions such as adsorption/desorption, precipitation/dissolution, water autoionization reaction, and electrolysis reaction were considered. For modeling purpose, a set of partial differential and algebraic equations were used to model the remediation process. The implicit finite difference numerical model showed a good capability of simulating the EKR process. The sensitivity analysis on the retardation and tortuosity factors represented that the retardation factor had a considerable effect on the pH and cadmium concentration profiles. Although tortuosity factor did not have a significant impact on the pH profile, it had a non-negligible effect on the cadmium concentration profile.

*Keywords:* Numerical Model; Finite Difference; Chemical Reaction; Electrokinetic; Cadmium; Sensitivity Analysis.

### 1. Introduction

Soil pollution is one of the most important concerns for environmentalists. Contaminants such as heavy metals, organic matters, and radionuclides threat soils and sediments. Various methods including bioremediation, thermal remediation, soil vapor extraction, soil washing, soil flushing, electrokinetic remediation (EKR) have been introduced to purify contaminated lands [1]. Among them, EKR has shown to be a practical method to remedy low permeable soils (e.g., clays and silts) [2–6]. In the EKR process, application of low direct current (DC) into the soil medium leads to contaminants transportation by different transport phenomena such as electro-migration, electroosmotic flow, and electrophoresis. Electro-migration is the transport of ions and charged complexes under an electric field which is the main mechanism for transportation of heavy metals. Electroosmotic flow is the movement of pore water through a porous medium of soils as a subsequence of the electric field, and it is the main factor for removing neutral contaminants (e.g., organic matter) [7]. Electrophoresis is the movement of charged colloidal size particles and bound contaminants under an electric field [8] and becomes significant in the EKR when surfactants are used to enhance the EKR process, or when the technique is employed in the remediation of slurries [9].

\* Corresponding author: [geo\\_miladrezaee@yahoo.com](mailto:geo_miladrezaee@yahoo.com)

 <http://dx.doi.org/10.28991/cej-030940>

➤ This is an open access article under the CC-BY license (<https://creativecommons.org/licenses/by/4.0/>).

© Authors retain all copyrights.

To understand the EKR's physicochemical phenomenon, mathematical models on the basis of the powerful theoretical framework are necessary. Mathematical models are essential to understand better processes that occur in the EKR and to allow predictions for the field-scale remediation [8]. Mathematical studies have been introduced to understand the feasibility of the models and to explain the fundamental theories. A chronological brief of numerical studies on EKR is being presented here. Chang et al. proposed a numerical model based on linear and non-linear retardation factor to consider adsorption of heavy metals in the remediation of copper and cadmium contaminated soil by EKR. They stated that their model based on Freundlich non-linear retardation factor had a good agreement with the experimental observation [10]. Kim et al. focused on simulating EKR of cadmium and lead contaminated kaolinites and they had reasonable agreements between numerical simulations and experimental tests [11, 12]. Park et al. developed a numerical model for remediation of phenol-contaminated kaolinite under an electric field, and the model results were consistent with the experimental results [13]. Amrate and Akretche provided a model for remediation of lead-contaminated soil under EKR which was enhanced by the disodium salt of ethylenediaminetetraacetic (EDTA) and they stated that the model results were in agreement with the experiment [14]. Mascia et al. proposed a numerical model with consideration of surface reactions to simulate remediation of cadmium-spiked kaolinite under EKR process [15]. Al-Hamdan and Reddy introduced a numerical model for the EKR of cadmium, chromium, and nickel contaminated kaolinite with considering chemical equilibrium reactions and their model was capable of simulating the experimental measurements [16]. Paz-Garcia et al. introduced a finite element numerical implementation for Nernst–Planck–Poisson system of equations for the EKR. They claimed that their model has a potential to predict the EKR process in both constant current density and the constant difference of voltage [17]. Miao and Pan built a numerical model to predict remediation of nuclear waste-contaminated soil under the direct current electric field, and the model results agreed with the tests' results [18]. Asadollahfardi et al. proposed an explicit finite difference model to simulate lead removal from kaolinite clay under EKR process and their simulation results were consistent with the experimental data [19]. Rezaee et al. presented a model to simulate remediation of zinc and copper contaminated soils under EKR process considering different chemical reactions and they reported that their model was capable of simulating the remediation process [20].

This paper presents a numerical model based on Crank-Nicolson method to simulate the EKR of a cadmium-contaminated kaolinite under an acid-enhanced condition. The realistic boundary conditions including the effect of flux and electrolysis reaction were considered in the model. Cadmium adsorption onto kaolinite surface was considered with the pH-dependent adsorption isotherm model in addition to precipitation and water chemical equilibrium. The final model compared with the existing data in the literature. Moreover, sensitivity analysis on the retardation and tortuosity factors were carried out to understand their effects on the model results. According to state of the art, simulation of acid-enhanced EKR by implicit finite difference method and taking into account realistic boundary conditions, chemical reactions, and conducting sensitivity analysis has not been investigated yet.

## 2. Materials and Method

### 2.1. Experimental Data

For validation of the numerical model, we used the EKR test reported by [21] for the removal of cadmium ions from water-saturated kaolinite. Figure 1 illustrates a schematic of the EKR batch system. The experimental study which was carried out by [21] is the kaolinite soil that was artificially contaminated by  $\text{Cd}(\text{NO}_3)_2$  solution. The experimental apparatus consists of four main parts; soil cell, electrode cells, anode and cathode electrolyte solution reservoirs and power supply. The soil cell dimension is  $9 \times 9 \times 15 \text{ cm}$  with a volume of  $1215 \text{ cm}^3$ . Soil cell ends has 81 holes (diameter;  $0.5 \text{ cm}$ ) to enhance uniform electroosmotic flow. At both sides of the soil cell, two sheets of filter paper were inserted to prevent flowing clay particles into the electrode cells. Constant-current was used in the test to keep the net rates of the electrolysis reactions constant. Table 1. presents a summary of the experimental data. Soil which was used in this experiment was commercial kaolinite soil was contaminated with Cd artificially. Kaolinite soil was contaminated with  $\text{Cd}(\text{NO}_3)_2$  solution. One liter of  $1000 \text{ mg L}^{-1}$  Cd(II) solution were prepared by dissolving  $2.801 \text{ g}$   $\text{Cd}(\text{NO}_3)_2$  in 1 L of distilled water. The contaminated kaolinite was allowed to settle down for more than 3 days to attain the uniform distribution of cadmium and to complete adsorption in the soil samples.

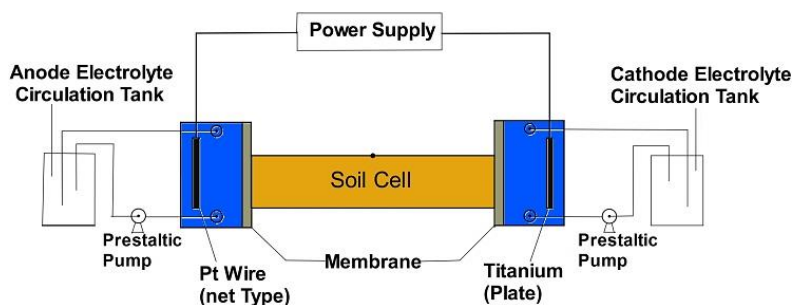


Figure 1. Schematic of the experimental apparatus [21]

**Table 1. Experimental data of the EKR test [21]**

Parameters	Value
Soil specimen	Kaolinite
Contaminants	Cd (NO <sub>3</sub> ) <sub>2</sub>
Initial Contaminant concentration (µg/g)	367
Initial soil pH	6
Applied current (A)	0.1
Applied Voltage (V)	17
Area of soil cell (cm <sup>2</sup> )	81
Length of the soil cell (cm)	15
Duration (h)	96

## 2.2. Chemical Species Transport Formulation

Different species transport phenomena in soils under electric field consist of mass fluxes generated by diffusion, electro-migration, electroosmotic flow, and electrophoresis. Several environmental variables affect the contribution of each flux to the total mass flux: soil mineralogy, pore fluid composition and conductivity, electrochemical properties of the present, generated and introduced species in the pore fluid, and porosity and tortuosity of the porous medium [9]. In the present study, electrophoresis is not considered in the model, because this process is taken into account when surfactants are used to enhance EKR. Moreover, the isothermal condition is considered; soil deformability is assumed to be negligible; soil medium is homogenous and saturated; the electrode dissolution is not taken into considering; redox reaction was considered merely at the electrodes; the movement of water under hydraulic gradient was not taken into consideration (no hydraulic head existed in the system); and model geometry was considered to be one-dimensional. A set of partial differential equations and algebraic equations are used to mathematically describe the transport of the target species, which in this case are: H<sup>+</sup>, OH<sup>-</sup>, Cd<sup>2+</sup>, and NO<sub>3</sub><sup>-</sup>. The flux of the chemical species through a soil due to the presence of different transport phenomena such as diffusion, electroosmosis, and electro-migration is [22-24]:

$$J_i = -D_i^{eff} \nabla c_i - c_i(u_i^{eff} + k_{eo}) \nabla \phi \tag{1}$$

$$D_i^{eff} = n\tau D_i \tag{2}$$

Where  $D_i^{eff}$  (m<sup>2</sup> s<sup>-1</sup>) is the effective diffusion coefficient,  $n$  (-) is the porosity of the soil,  $\tau$  is the tortuosity factor,  $u_i^{eff}$  (m<sup>2</sup> V<sup>-1</sup> s<sup>-1</sup>) is the effective ionic mobility,  $k_{eo}$  (m<sup>2</sup> V<sup>-1</sup> s<sup>-1</sup>) is the electroosmotic permeability,  $\phi$  (V) is the electrical potential, and  $c_i$  (mol m<sup>-3</sup>) is the concentration. For estimating effective ionic mobility the Nernst-Einstein relation was used [23-25]:

$$u_i^{eff} = \frac{z_i F}{RT} D_i^{eff} \tag{3}$$

Where  $z_i$  is the ionic charge of the species;  $F$  (C mol<sup>-1</sup>) is the Faraday constant;  $R$  (J K<sup>-1</sup> mol<sup>-1</sup>) is the ideal gas constant, and  $T$  (K) is the absolute temperature. By imposing mass conservation law, a system of differential and algebraic equations consisting  $N$  mass balance could describe the concentration profiles in the electrolyte, one for each chemical species and the electroneutrality condition, which are presented in equations 4 and 5,

$$n \frac{\partial c_i}{\partial t} = -\nabla \cdot J_i + nG_i \ ; \ i = 1, 2, \dots, N \tag{4}$$

$$\sum_{i=1}^N c_i z_i = 0 \tag{5}$$

$G_i = G_i^{ad} + G_i^p + G_i^{aq}$  in which  $G_i$  (mol m<sup>-3</sup> s<sup>-1</sup>) is consumption\production  $i$ th aqueous chemical species due to chemical reactions (as e.g. adsorption, precipitation, and ionization). Where  $G_i^{aq}$  is the production rate of the  $i$ th aqueous chemical species because of an aqueous phase reaction; and  $G_i^{ad}$  is the production rate of the  $i$ th aqueous chemical species due to an adsorption reaction; and  $G_i^p$  is the production rate of the  $i$ th aqueous chemical species because of a precipitation reaction.

## 2.3. Chemical Reaction

### 2.3.1. Electrolysis Reaction

In the model, water electrolysis reaction was considered, water oxidation at the anode and reduction at the cathode, as



Where  $E^0$  is the standard redox potential of the half reaction. The electrolysis reactions produce the injection of protons and hydroxide ions from the anode and the cathode, respectively [8, 17]. No other competitive electrode reactions were taken into consideration in the model.

**2.3.2. Adsorption Reaction**

Adsorption is the net accumulation of chemical species at the interface between a solid phase and fluid phase [26]. It is considered that the adsorption of heavy metal ions and complexes on clay minerals occurs as a result of ion exchange, surface complexation, hydrophobic interaction, and electrostatic interaction [27]. Factors such as pH, nature, and concentration of a substrate and adsorbing ion, ionic strength, and the presence of complexing ions, affect the extent of an adsorption [28, 29].

In the present study, cadmium and proton adsorption was taken into account due to their positive electric charge and  $H^+$  and  $NO_3^-$  are the negative electric charge and considering adsorption for them is meaningless. A linear function is the simplest and most widely used adsorption isotherm equation was utilized to describe the adsorption of proton onto the kaolinite surface in the model. The adsorption isotherm equation is conventionally expressed regarding the distribution coefficient:

$$G_i^{ad} = -\frac{\rho}{n} \frac{\partial c_i^{ad}}{\partial t} = -\frac{\rho}{n} \frac{\partial c_i^{ad}}{\partial c_i} \frac{\partial c_i}{\partial t} \tag{8}$$

$$\frac{\partial c_i^{ad}}{\partial c_i} = K_{di} \tag{9}$$

$$R_{di} = 1 + \frac{\rho K_{di}}{n} \tag{10}$$

Where  $c_i^{ad}$  (mol  $kg^{-1}$ ) is the amount of solute absorbed/adsorbed onto a unit weight of solid,  $c_i$  (mol  $m^{-3}$ ) is the concentration of solute,  $K_{di}$  ( $m^3 kg^{-1}$ ) is the distribution coefficient,  $\rho$  is the bulk dry density of the soil and  $R_{di}$  is the retardation factor. Yet, adsorption reaction for cadmium and proton are interactive when pH value is the effective parameter in sorption species on a soil. For considering cadmium adsorption isotherm as a function of soil pH in different concentrations, an empirical model was used to consider cadmium adsorption onto kaolinite surface.

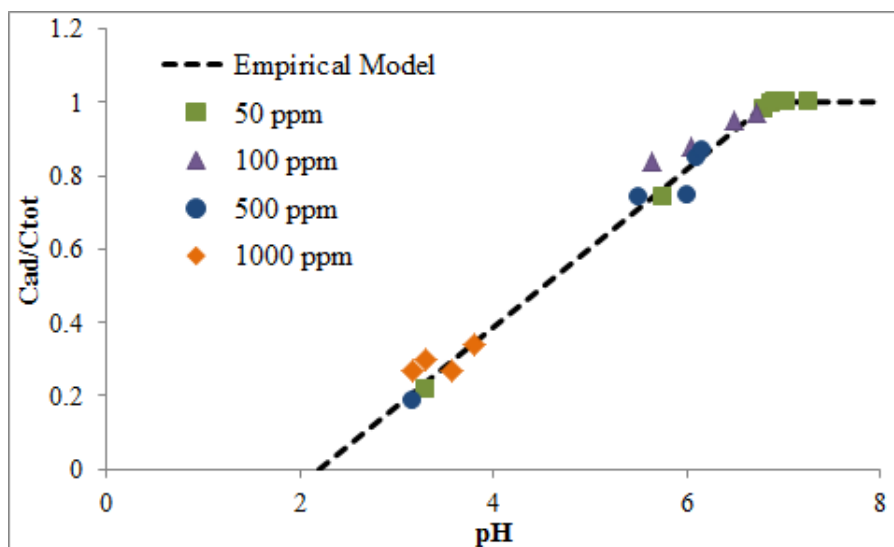
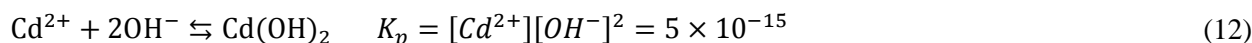


Figure 2. Experimental result of cadmium adsorption isotherm onto kaolinite in different pH values [12]

**2.3.3. Water Chemical Equilibrium and Precipitation Reaction**

Aqueous and precipitation reactions in the models were considered by Equations 12 and 13, respectively,



$K_w$  is the water equilibrium constant, and  $K_p$  is the solubility product equilibrium constant of the precipitation reaction.

## 2.4. Finite Difference Implementation and Model Procedure

For each ion, except nitrate that its concentration is calculated by using an algebraic equation, two boundary conditions and one initial condition were introduced. The electric field was set constant with time [15, 16, 19, 20]; therefore, the transport equation for each chemical species along with appropriate boundary conditions at the electrodes for each ion is presented.

Cadmium:

$$n \frac{\partial c_{Cd}}{\partial t} = D_{Cd}^{eff} \frac{\partial^2 c_{Cd}}{\partial x^2} + (u_{Cd}^{eff} + k_{eo}) \frac{\partial c_{Cd}}{\partial x} \frac{\partial \phi}{\partial x} + n(G_{Cd}^p + G_{Cd}^{ad}) \quad (13)$$

$$-D_{Cd}^{eff} \frac{\partial c_{Cd}}{\partial x} + (k_{eo} + u_{zn}^{eff}) \left(-\frac{\partial \phi}{\partial x}\right) c_{Cd} \Big|_{x=Anode} = 0 \quad (14)$$

$$-D_{Cd}^{eff} \frac{\partial c_{Cd}}{\partial x} + (k_{eo} + u_{Cd}^{eff}) \left(-\frac{\partial \phi}{\partial x}\right) c_{Cd} \Big|_{x=Cathode} = c_{Cd} k_{eo} \left(-\frac{\partial \phi}{\partial x}\right) \quad (15)$$

Proton:

$$nR_{dH^+} \frac{\partial c_{H^+}}{\partial t} = D_{H^+}^{eff} \frac{\partial^2 c_{H^+}}{\partial x^2} + (u_{H^+}^{eff} + k_{eo}) \frac{\partial c_{H^+}}{\partial x} \frac{\partial \phi}{\partial x} + nG_{H^+}^{aq} \quad (16)$$

$$-D_{H^+}^{eff} \frac{\partial c_{H^+}}{\partial x} + (k_{eo} + u_{H^+}^{eff}) \left(-\frac{\partial \phi}{\partial x}\right) c_{H^+} \Big|_{x=Anode} \quad (17)$$

$$= c_0^{H^+} k_{eo} \left(-\frac{\partial \phi}{\partial x}\right) + \frac{I}{F}$$

$$-D_{H^+}^{eff} \frac{\partial c_{H^+}}{\partial x} + (k_{eo} + u_{H^+}^{eff}) \left(-\frac{\partial \phi}{\partial x}\right) c_{H^+} \Big|_{x=Cathode} \quad (18)$$

$$= c_{H^+} k_{eo} \left(-\frac{\partial \phi}{\partial x}\right)$$

Hydroxide:

$$n \frac{\partial c_{OH^-}}{\partial t} = D_{OH^-}^{eff} \frac{\partial^2 c_{OH^-}}{\partial x^2} + (u_{OH^-}^{eff} + k_{eo}) \frac{\partial c_{OH^-}}{\partial x} \frac{\partial \phi}{\partial x} + n(G_{OH^-}^p + G_{OH^-}^{aq}) \quad (19)$$

$$-D_{OH^-}^{eff} \frac{\partial c_{OH^-}}{\partial x} + (k_{eo} + u_{OH^-}^{eff}) \left(-\frac{\partial \phi}{\partial x}\right) c_{OH^-} \Big|_{x=Anode} = c_0^{OH^-} k_{eo} \left(-\frac{\partial \phi}{\partial x}\right) \quad (20)$$

$$-D_{OH^-}^{eff} \frac{\partial c_{OH^-}}{\partial x} + (k_{eo} + u_{OH^-}^{eff}) \left(-\frac{\partial \phi}{\partial x}\right) c_{OH^-} \Big|_{x=Cathode} = c_{OH^-} k_{eo} \left(-\frac{\partial \phi}{\partial x}\right) - \frac{I}{F} \quad (21)$$

where  $I$  (A m<sup>-2</sup>) is the electric current density;  $c_0^{H^+}$  is the concentration of proton in the anode compartment;  $c_0^{OH^-}$  is the concentration of hydroxide in the anode compartment; and  $R_{dH}$  is the proton retardation factor. In order to generate boundary conditions, it was assumed that whole electric current was expended in the generation of H<sup>+</sup> at the anode and OH<sup>-</sup> at the cathode. By imposing electroneutrality into the system of equations, it is possible to achieve NO<sub>3</sub><sup>-</sup> concentration at each time and space by:

$$C_{NO} = -\frac{\sum_{j=1}^3 Z_j C_j}{Z_{NO}} \quad (22)$$

The initial condition for cadmium, proton, and hydroxide are represented in Table 2.

**Table 2. Initial condition of target species**

Species	Initial condition
Cadmium	8.9×10 <sup>-3</sup> (mol/m <sup>3</sup> )
Proton	10 <sup>-6</sup> (mol/lit)
Hydroxide	10 <sup>-8</sup> (mol/lit)

The transport equation for each ion should be solved by using appropriate initial condition, and the chemical reactions should be satisfied at each time step, then equilibrium concentration of each chemical species goes to transport formulation to obtain the concentrations at the next time step. The finite difference formulation which was used to solve the transport equation is completely described in [20]. The electroosmotic permeability in soils is in the range of 10<sup>-5</sup> to 10<sup>-4</sup> cm<sup>2</sup> s<sup>-1</sup> V<sup>-1</sup> [22]. In our case, we set electroosmotic permeability equal to 5×10<sup>-9</sup> (m<sup>2</sup> V<sup>-1</sup> s<sup>-1</sup>). Tortuosity factor for

kaolinite varies over a range of 0.12-0.5 [23]. We considered the tortuosity factor equal 0.15 and retardation factor equal to 7 according to sensitivity analysis and we used characteristics from Table 3 in our simulation.

**Table 3. parameters used in Numerical Analysis**

Parameter	Value	Reference
Length of soil cell (cm)	15	[21]
Time of simulation (hr)	96	[21]
Spatial increment (mm)	0.1	-
Time increment (s)	10	-
Porosity	0.48	[12]
Cation exchange capacity (CEC) (mg kg <sup>-1</sup> )	3280	[12]
$D_i$ of Cd <sup>2+</sup> (m <sup>2</sup> s <sup>-1</sup> )	$7.19 \times 10^{-10}$	[30]
$D_i$ of H <sup>+</sup> (m <sup>2</sup> s <sup>-1</sup> )	$93.1 \times 10^{-10}$	[30]
$D_i$ of OH <sup>-</sup> (m <sup>2</sup> s <sup>-1</sup> )	$52.7 \times 10^{-10}$	[30]
$D_i$ of NO <sub>3</sub> <sup>-</sup> (m <sup>2</sup> s <sup>-1</sup> )	$19 \times 10^{-10}$	[30]
Applied electric field (V)	17	[21]

At each time step chemical reactions should be solved to find equilibrium value of each chemical species concentration. At first step transport equations are solved according to initial conditions by finite difference method to find concentrations at the next time step, then water chemical equilibrium, precipitation, and pH-dependent adsorption isotherm model are solved to find species equilibrium concentration and these concentrations go to transport equation to find species concentration at the new time step. This procedure should be continued to find all concentrations. Figure 3 shows the numerical procedure which was used to simulate the EKR process.

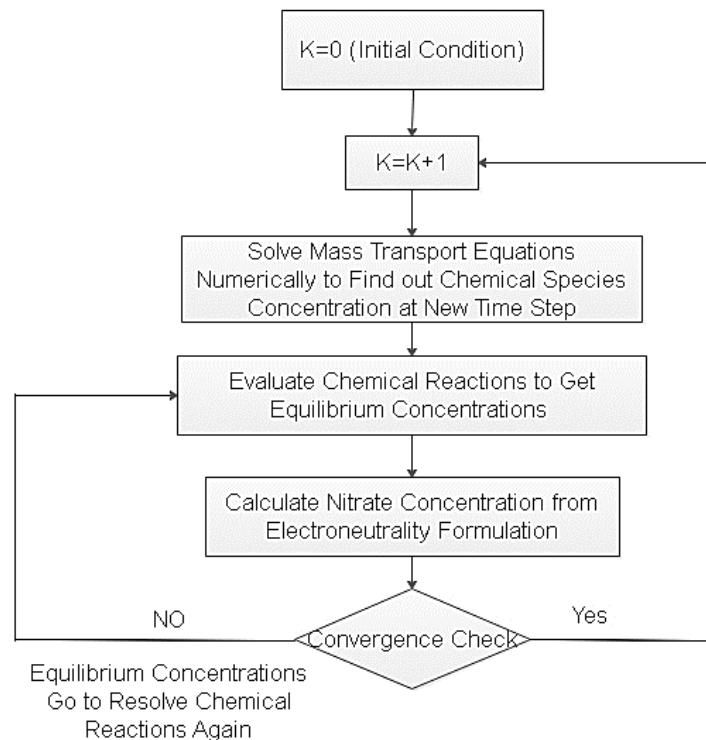


**Figure 3. Visual description of numerical procedure to simulate EKR process**

**2.5. Analysis Model Efficiency**

The coefficient of determination ( $R^2$ ) and index of agreement (IA) indicate the accuracy of simulation results. To illustrate the accuracy and efficiency of the models,  $R^2$  and IA were calculated between our numerical simulation results and the experimental measurement. The  $R^2$  and IA values are between zero to one. When the  $R^2$  and IA approach to one the model is well developed. The  $R^2$  and IA formulations are:

$$R^2 = \left( \frac{\sum_{i=1}^n (O_i - \bar{O})(P_i - \bar{P})}{\sqrt{\sum_{i=1}^n (O_i - \bar{O})^2} \sqrt{\sum_{i=1}^n (P_i - \bar{P})^2}} \right)^2 \quad (23)$$

$$IA = 1 - \frac{\sum_{i=1}^n (O_i - P_i)^2}{\sum_{i=1}^n (|P_i - \bar{O}| + |O_i - \bar{O}|)^2} \quad (24)$$

where O is the experimental measurement,  $\bar{O}$  is the mean value of O, P is the numerical simulation result and  $\bar{P}$  is the mean value of P.

### 3. Results and Discussion

#### 3.1. Comparison between the Model Prediction and Experimental Result

Figure 4 indicates the comparison between the model prediction and the experimental pH measurements. Due to the electrolysis reaction, proton and hydroxide ions are generated in the anode and the cathode chambers, respectively [31, 32]. These ions move into the soil medium and cause acid and base front movement. In acid-enhanced tests, by dropping acid into the cathode chamber, pH in the cathode chamber does not increase. In the acidic condition in the cathode chamber OH<sup>-</sup> ions are neutralized. In the modeled system sulphuric acid was used to enhance the remediation process, so in the cathode chamber, hydroxide reacts with sulphuric acid and produces water and SO<sub>4</sub><sup>2-</sup>. In this content, the acid front movement is prevented and pH near the cathode does not increase, which results in more efficient remediation process by reducing adsorption and precipitation of cadmium ions. Close to the anode cell the model and the test's result illustrate acidic condition which is due to high concentration of proton ions in this zone. Close to the cathode, pH tends to the initial soil pH, because it takes time for proton ions to travel to cathode zone, so pH in this zone is not acidified as anode zone. R<sup>2</sup> and IA were calculated between the model result and pH measurement along the soil. The R<sup>2</sup> and IA calculation for the third day are 0.99 and 0.98 and for the fourth day are 0.99 and 0.99 which shows good agreement between the present model and experimental measurements.

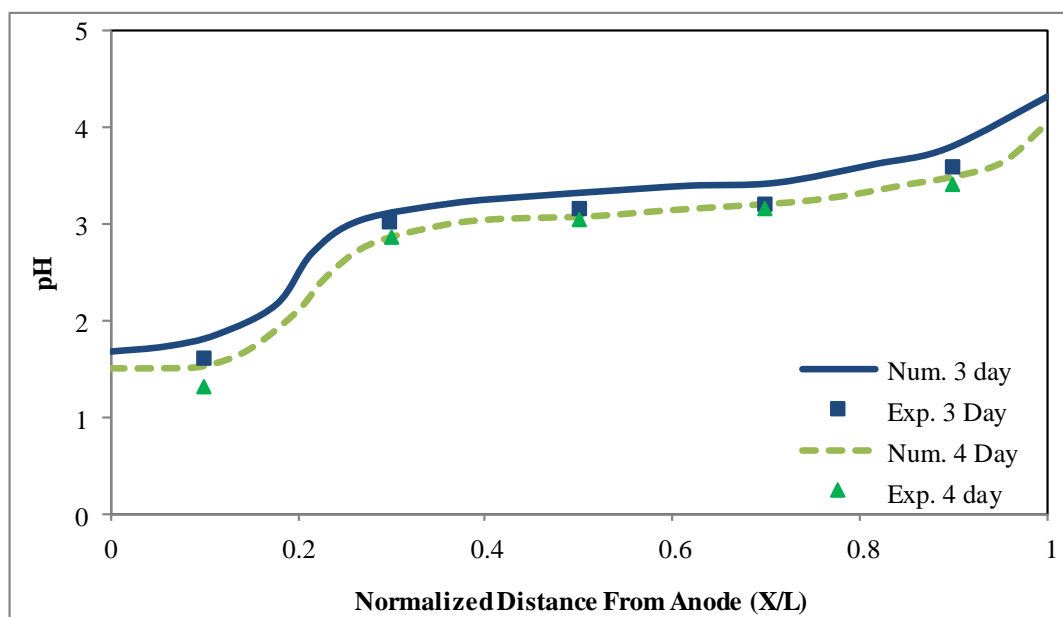


Figure 4. Predicted and measured pH along the soil cell

Figure 5 describes the comparison between the cadmium concentration prediction and the experimental data. By running the program and then decreasing pH, the cadmium ions desorbed from the kaolinite surface and transported across the soil medium. Owing to the acid enhancement strategy, the whole of the soil medium was acidified based on the experiment and the model (Figure 4). Therefore, less cadmium accumulation is observed in comparison with unenhanced tests because of less adsorption and precipitation [33]. In the acid-enhanced EKR test, high efficiency in remediation of cadmium is observable, because cadmium ions are mostly soluble and could transport in soil media. According to Figure 5, the model result is consistent with the experimental data and shows a good capability for simulating the cadmium concentration profile in the soil. The R<sup>2</sup> and IA calculation between the proposed model result and the experimental cadmium concentration profile show reasonable agreement between the model and the experiment. In the third day R<sup>2</sup> and IA are equal 0.83 and 0.82 and for the fourth day, R<sup>2</sup> and IA are equal to 0.65 and 0.8 which

show reasonable agreement between the model and the experiment.

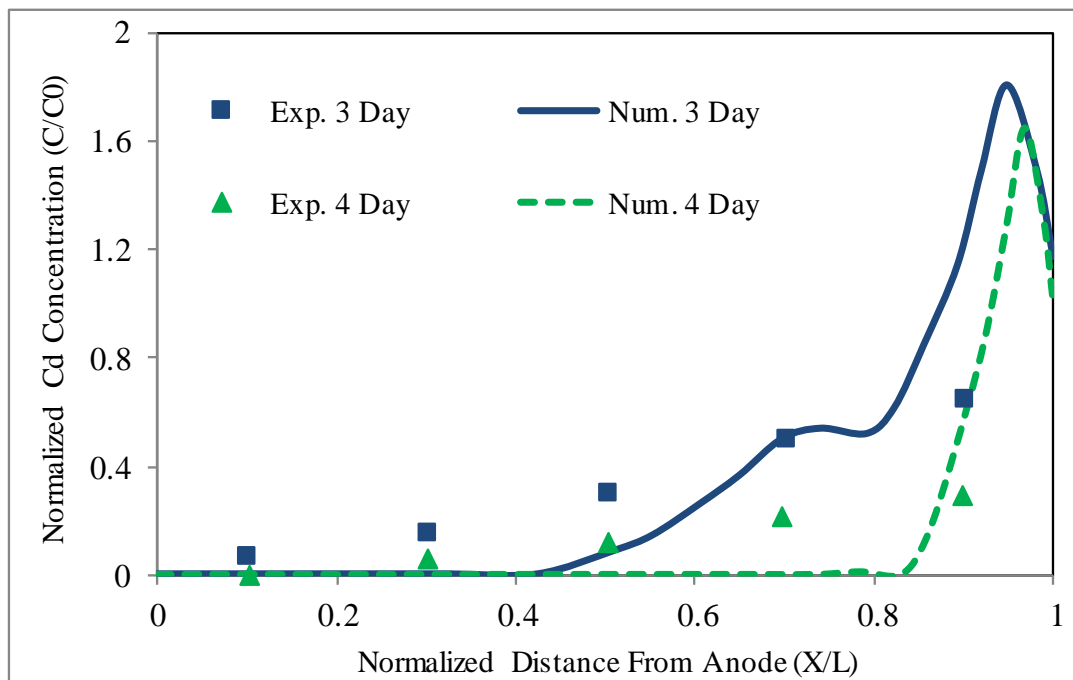


Figure 5. Predicted and measured cadmium concentration profile

### 3.2. Sensitivity Analysis

In our study, the retardation and tortuosity factors were considered as the fitting parameters (or degree of freedom) to achieve a good agreement between the experimental and the simulation results. Other input parameters have a specific value and uncertainty is existed for tortuosity and retardation factor values. Consequently, we carried out a sensitivity analysis on these parameters to find out their effects on the model. In the first phase, we increased or decreased the retardation factor by 20%, while the other input parameters were kept unchanged, then the role of retardation factor in the model results was investigated. Figures 6 and 7 indicate the effect of using different retardation factors on the pH profile after three and four days of treatments, respectively. When the retardation factor was set equal to 5.6, the acid front movement accelerated and this means that proton ions could transport more easily in comparison with using retardation factor equal to 7 and the model for three and four days of treatment represented overestimation for the pH prediction. When retardation factor was equal to 8.4, the acid front movement was retarded. Consequently, the model underestimated acid front movement and simulated the pH profile equal to the initial soil pH near the cathode after three and four days of treatment.

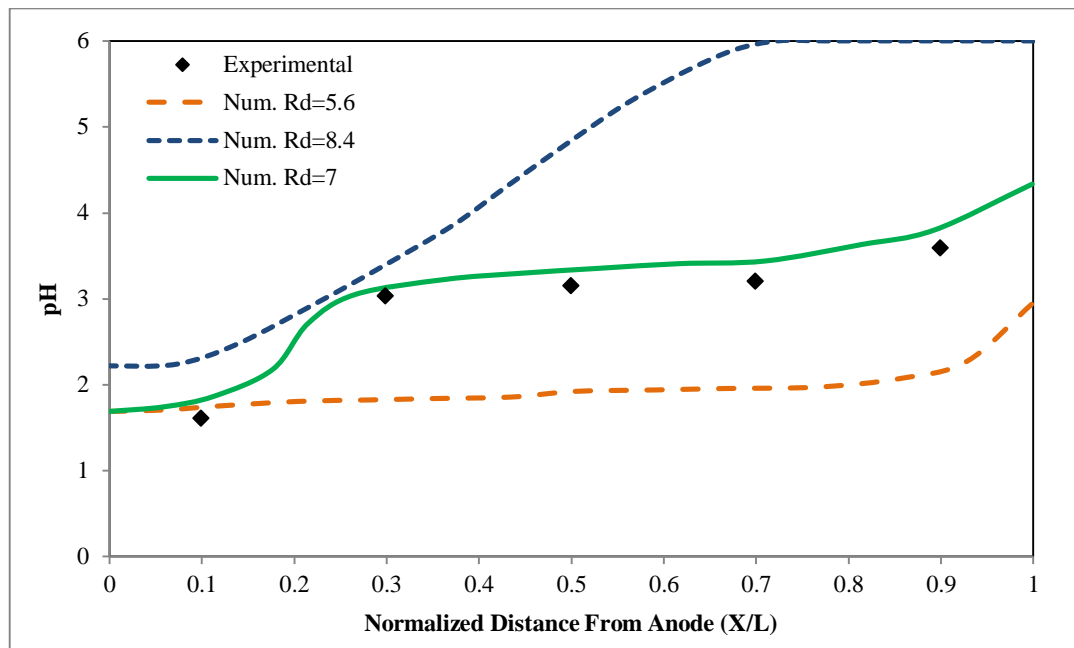


Figure 6. Effect of changing the retardation factor on the pH prediction after 3 days of treatment

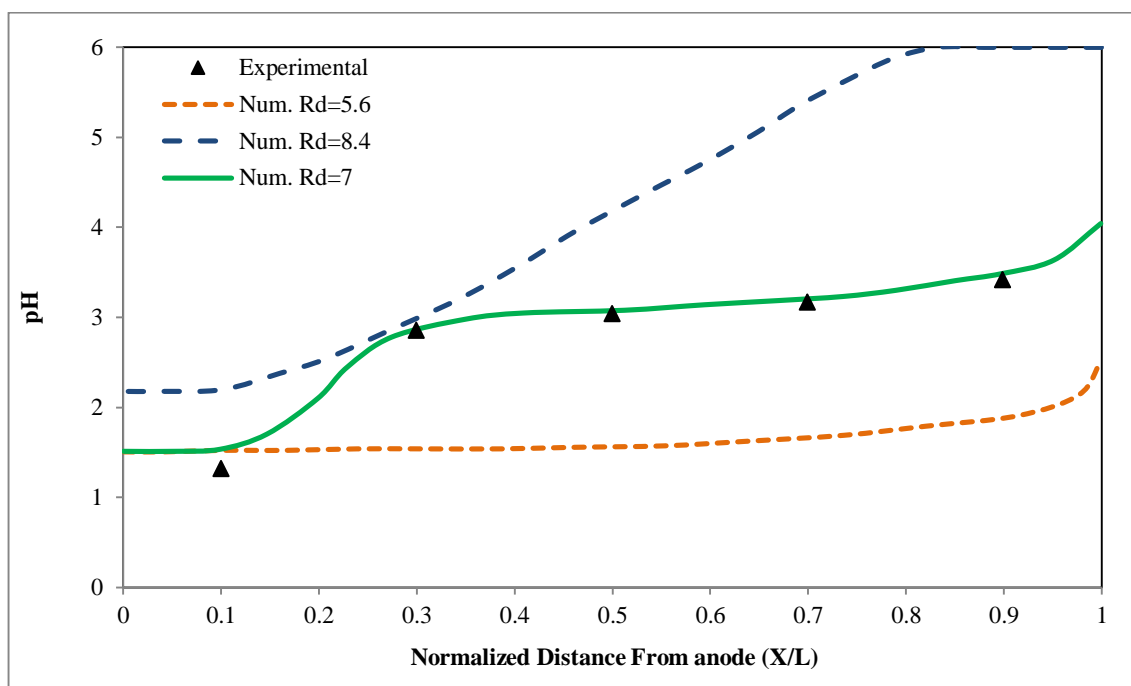


Figure 7. Effect of changing the retardation factor on the pH prediction after 4 days of treatment

Figures 8 and 9 present the effect of changing the retardation factor on the cadmium concentration profile after three and four days of treatment, respectively. As illustrated in Figures 6 and 7 by using retardation factor equal to 5.6 the model overestimated the acid front movement. Therefore, in the strong acidic condition, cadmium ions could transfer in the soil with less interaction with soil surface and other ions (less adsorption and precipitation). Because, the cadmium adsorption is interactive with the proton concentration and according to the pH-dependent adsorption isotherm model, less cadmium accumulation was observed by the model (Figure 8 and 9). In addition, as Figure 6 and 7 depict, when retardation factor was considered equal to 8.4 after three and four days of treatment the model underestimated the acid front movement and displayed the soil pH equal to the initial amount. This condition resulted in more adsorption and precipitation, and the model underestimated the cadmium removal (Figure 8 and 9).

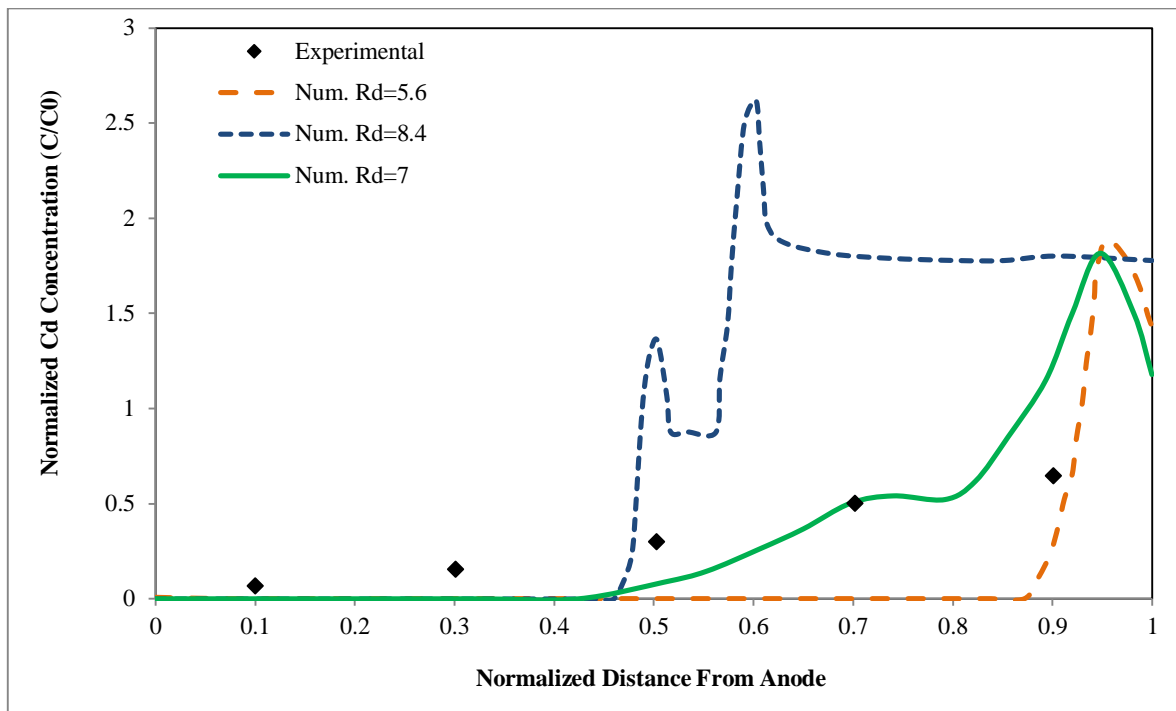


Figure 8. Effect of changing the retardation factor on the cadmium concentration profile after 3 days of treatment

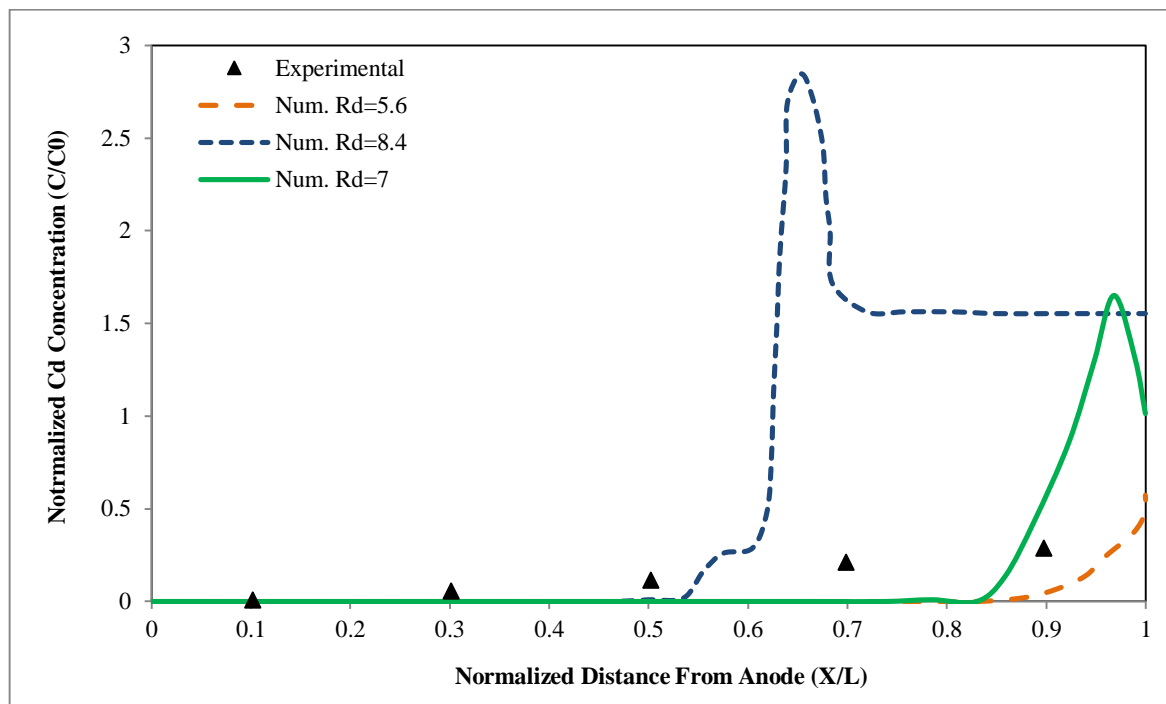


Figure 9. Effect of changing the retardation factor on the cadmium concentration profile after 4 days of treatment

In the second phase of the sensitivity analysis, we increased or decreased the tortuosity factor by 20%, while the other input parameters were kept unchanged, then the role of tortuosity factor in the model results was investigated. As Figure 10 and 11 demonstrate when tortuosity factor was set equal to 0.12 and 0.18 the model did not show a considerable change in the pH profile. The tortuosity factor did not have a significant effect on the pH profile prediction.

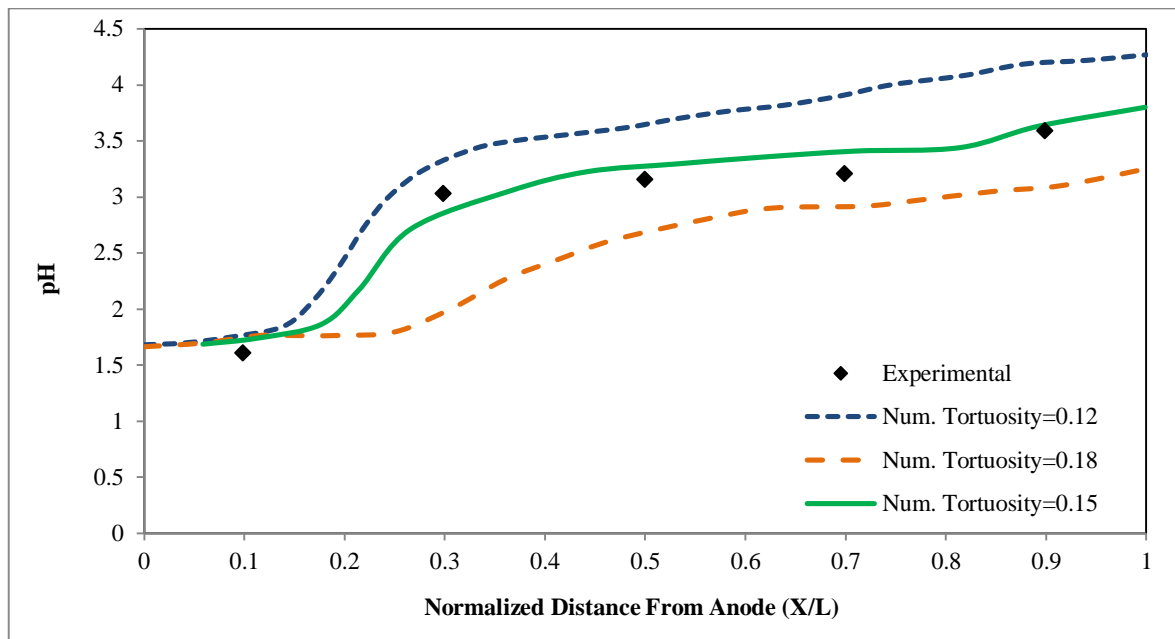


Figure 10. Effect of changing tortuosity factor on the pH profile after 3 days of treatment

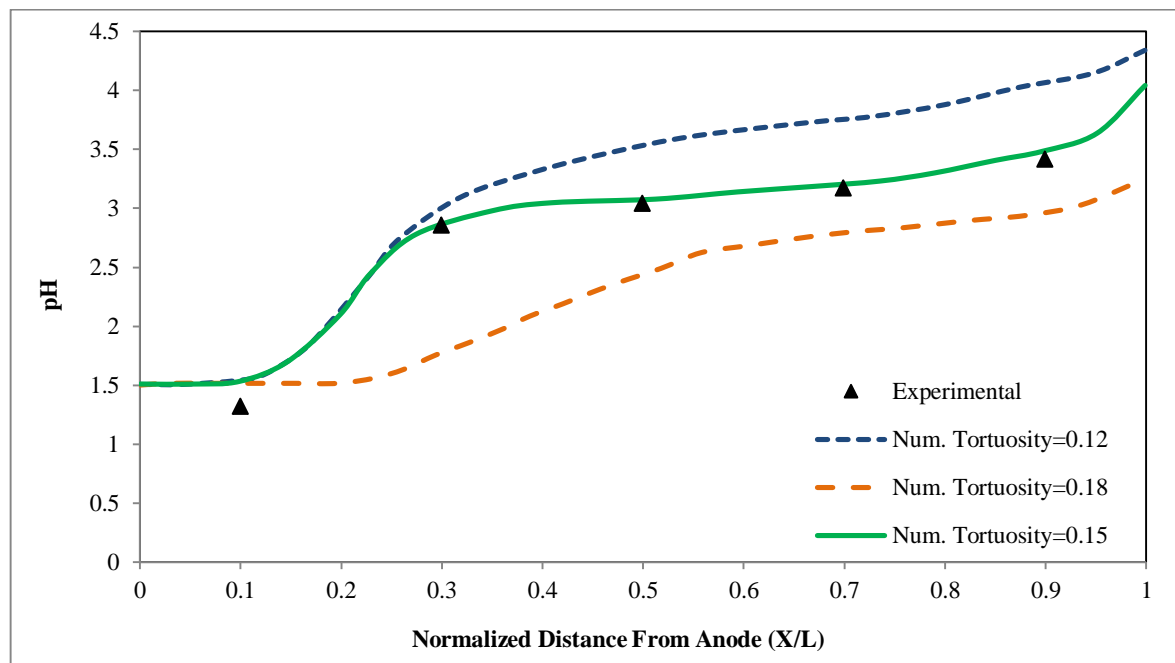


Figure 11. Effect of changing tortuosity factor on the pH profile after 4 days of treatment

Figures 12 and 13 depict the effect of changing tortuosity factor on the cadmium concentration profile after three and four days of treatment, respectively. By increasing the tortuosity factor ( $\tau = 0.18$ ), the cadmium's effective ionic mobility is increased and the model overestimated cadmium removal. Moreover, when the tortuosity factor was taken into account equal to 0.12, the model underestimated the cadmium removal, because the cadmium's effective ionic mobility decreased. This change in the cadmium concentration profile is due to the fact that the tortuosity factor has a

direct impact on the cadmium's ionic mobility.

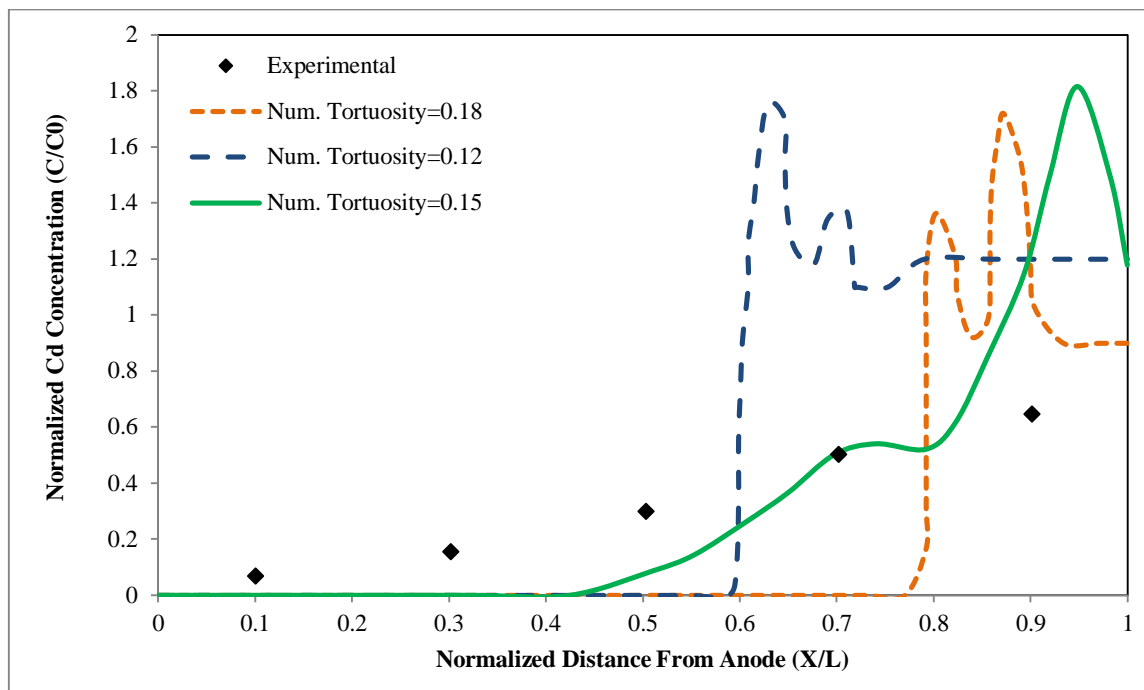


Figure 12. Effect of changing the tortuosity factor on the cadmium concentration profile after 3 days of treatment

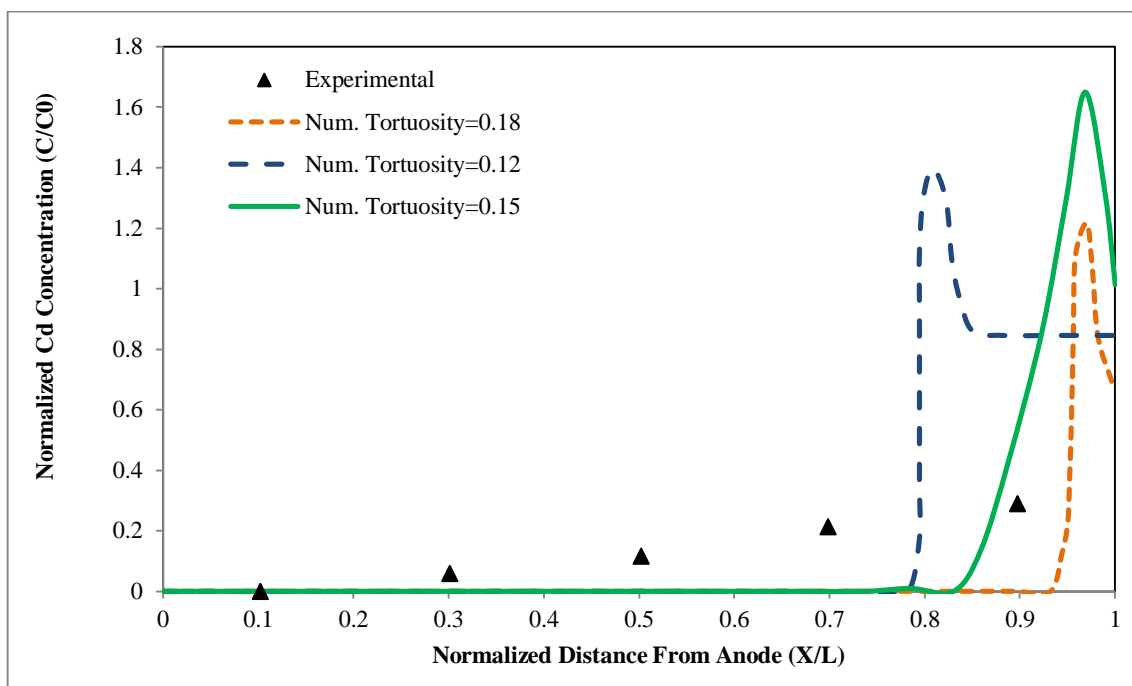


Figure 13. Effect of changing the tortuosity factor on the cadmium concentration profile after 4 days of treatment

#### 4. Conclusion

This paper presents a numerical model on the basis of the implicit finite difference considering chemical reactions consisting pH-dependent adsorption isotherm, water autoionization, precipitation and electrolysis in the electrode cells to model the acid-enhanced EKR of a cadmium-contaminated soil. Considering the results and discussion, we summarized the conclusions as follows:

Cadmium concentration and pH prediction along the soil had a reasonable agreement with the experimental data which represent the efficiency of the model to simulate the modeled system. The consequence of sensitivity analysis on the retardation factor showed that this parameter had a significant effect on the pH profile and the cadmium concentration

prediction. Moreover, the result of the sensitivity analysis on the tortuosity factor indicated that this parameter did not have a significant effect on the pH profile prediction. Conversely, tortuosity factor had a non-negligible effect on the cadmium concentration profile simulated by the model.

## 5. References

- [1] Virkutyte, J. Sillanpää, M. and Latostenmaa, P. Electrokinetic soil remediation - Critical overview, *Sci. Total Environ.*, 289 (2002): 97–121. doi: 10.1016/s0048-9697(01)01027-0.
- [2] Acar, Y.B. and Alshawabkeh, A.N. Electrokinetic remediation. II: Theoretical Study, *J. Geotech. Eng.*, 122 (1996): 173–185. doi: 10.1061/(asce)0733-9410(1996)122:3(173).
- [3] Kim, S.O. Kim, W.S. and Kim, K.W. Evaluation of electrokinetic remediation of arsenic-contaminated soils, *Environ. Geochem. Health*, 27 (2005): 443–453. doi:10.1007/s10653-005-2673-z.
- [4] Al-Shahrani, S.S. and Roberts, E.P.L. Electrokinetic removal of caesium from kaolin, *J. Hazard. Mater*, 122 (2005): 91–101. doi:10.1016/j.jhazmat.2005.03.018.
- [5] Saeedi, A. Li, L.Y. and Gharehtapeh, A. Effect of alternative electrolytes on enhanced electrokinetic remediation of hexavalent chromium in clayey soil. *Int. J. Environ. Res.* 7(2013): 39-50. doi:10.22059/IJER.2012.584.
- [6] Reddy, K.R. Maturi, K. and Cameselle, C. Sequential Electrokinetic Remediation of Mixed Contaminants in Low Permeability Soils. *Journal of environmental engineering.* 135 (2009): 989–999. doi:10.1061/(asce)ee.1943-7870.0000077.
- [7] Vereda-Alonso, C. Rodríguez-Maroto, J. M. García-Delgado, R. A. Gómez-Lahoz, C. and García-Herruzo, F. Two-dimensional model for soil electrokinetic remediation of heavy metals: Application to a copper spiked kaolin, *Chemosphere*, 54(2004): 895–903. doi: 10.1016/j.electacta.2006.01.087.
- [8] Reddy, K.R. and Cameselle, C. *Electrochemical Remediation Technologies for polluted soils, sediments and groundwater*, Wiley, 2009. doi: 10.1002/9780470523650.
- [9] Acar Y. B. and Alshawabkeh, A. N. Principles of electrokinetic remediation, *Environ. Sci. Technol.*, 27(1993): 2638–2674. doi: 10.1021/es00049a002.
- [10] Chang, C. M. Wang, M. K. Chang, T. W. Lin, C. and Chen, Y. R. Transport modeling of copper and cadmium with linear and nonlinear retardation factors, *Chemosphere*, 43(2001): 1133–1139. doi: 10.1016/s0045-6535(00)00176-4.
- [11] Kim, S. Kim, J. Kim, K. and Yun, S. Models and Experiments on Electrokinetic Removal of Pb(II) from Kaolinite Clay, *Separation Science and Technology*, 39 (2004): 1927–1951. doi: 10.1081/ss-120030775 .
- [12] Kim, S.O. Kim, J. J. Yun, S. T. and Kim, K. W. Numerical and experimental studies on Cadmium(II) transport in kaolinite clay under electrical fields, *Water, Air Soil Pollut.* 150 (2003): 135–162. doi: 10.1023/A:102618180
- [13] Park, J. S. Kim, S. O. Kim, K. W. Kim, B. R. and Moon, S. H. Numerical analysis for electrokinetic soil processing enhanced by chemical conditioning of the electrode reservoirs, *J. Hazard. Mater.*, 99 (2003): 71–88. doi: 10.1016/s0304-3894(03)00038-4.
- [14] Amrate S. and Akretche, D. E. Modeling EDTA enhanced electrokinetic remediation of lead contaminated soils, *Chemosphere*, 60 (2005): 1376–1383. doi: 10.1016/j.chemosphere.2005.02.021.
- [15] Mascia, M. Palmas, S. Polcaro, A. M. Vacca, A. and Muntoni, A. Experimental study and mathematical model on remediation of Cd spiked kaolinite by electrokinetics, *Electrochim. Acta*, 52(2007): 3360–3365. doi: 10.1016/j.electacta.2006.04.066 .
- [16] Al-Hamdan A. Z. and Reddy, K. R. Electrokinetic Remediation Modeling Incorporating Geochemical Effects, *J. Geotech. Geoenvironmental Eng.*, 134 (2008): 91–105. doi: 10.1061/(asce)1090-0241(2008)134:1(91)
- [17] Paz-García, J. M. Johannesson, B. Ottosen, L. M. Ribeiro, A. B. and Rodríguez-Maroto, J. M. Modeling of electrokinetic processes by finite element integration of the Nernst-Planck-Poisson system of equations, *Sep. Purif. Technol.* 79(2011): 183–192. doi: 10.1016/j.seppur.2011.02.023.
- [18] Miao T. and Pan, T. A Multiphysics Model for Evaluating Electrokinetic Remediation of Nuclear Waste-Contaminated Soils, *Water, Air, Soil Pollut.* 226(2015): 77. doi: 10.1007/s11270-014-2292-3.
- [19] Asadollahfardi, G. Rezaee, M. and Tavakoli Mehrjardi, G. Simulation of Unenhanced Electrokinetic Process for Lead Removal from Kaolinite Clay, *Int. J. Civ. Eng.*, 14 (2016): 263-270. doi: 10.1007/s40999-016-0049-7.
- [20] Rezaee, M. Kargar, P. and Mohammad Hosseini, A. Electrokinetic Remediation of Zinc and Copper Contaminated Soil : A Simulation-based Study. *Civil Engineering Journal.* 3(2017): 690–700. doi: 10.21859/cej-03096.
- [21] Kim, S. O. Moon, S. H. and Kim, K. W. Removal of Heavy Metals from Soils using Enhanced Electrokinetic Soil Processing, *Water. Air. Soil Pollut.* 125(2001): 259–272. doi: 10.1023/A:1005283001877.

- [22] Mitchell, J. K. *Fundamentals of Soil Behavior*. Wiley, 1993.
- [23] Alshawabkeh, A.N. *Theoretical and Experimental Modeling of Removing Contaminants from Soils by an Electric Field*, PhD thesis, The Louisiana State University, 1994.
- [24] Probstein, R.F. *Physicochemical Hydrodynamics – An Introduction*. Wiley 1994.
- [25] Holmes, P. *Electrochemistry of Semiconductors*. Academic Press, 1962.
- [26] Sposito, G. *The Chemistry of Soils*, Oxford University Press, 1989.
- [27] Hizal, J. and Apak, R. Modeling of cadmium(II) adsorption on kaolinite-based clays in the absence and presence of humic acid, *Appl. Clay Sci.*, 32 (2006): 232–244. doi: 10.1016/j.clay.2006.02.002.
- [28] Srivastava, P. Singh, B. and Angove, M. Competitive adsorption behavior of heavy metals on kaolinite, *J. Colloid Interface Sci.*, 290 (2005), 28–38. doi: 10.1016/j.jcis.2005.04.036 .
- [29] Ikhsan, J. Johnson, B. and Wells, J. A Comparative Study of the Adsorption of Transition Metals on Kaolinite, *J. Colloid Interface Sci.*, 217 (1999): 403–410. doi: 10.1006/jcis.1999.6377.
- [30] Lide, D. R. *CRC Handbook of Chemistry and Physics*. CRC Press 2009. doi: 10.1021/ja906434c
- [31] Rezaee, M. *Numerical Modeling of Electrokinetic Remediation of Heavy Metal Contaminated Kaolinite Soil*. MS.c. Thesis, Kharazmi University, 2014.
- [32] Rezaee, M. Asadollahfardi, G. and Gisel, M. Finite Difference Modeling of Electro-kinetic Process to Remove Lead from Kaolinite, *First National Conference on Soil Mechanics and Foundation Engineering*, 2014.
- [33] Asadollahfardi, G. Nasrollahi Gisel, M. and Rezaee, M. *Electrochemical Remediation Technology : Fundamentals, Benefits and Challenges* Third international symposium on environmental and water resource engineering, 2015.